DEFENCE R&D DÉFENSE

A Novel Approach for the Wigner Distribution Formulation of the Optimum Detection Problem for a Discrete-Time Chirp Signal

T. Thayaparan and A. Yasotharan

Defence R&D Canada
TECHNICAL MEMORANDUM
DREO TM 2001-141
November 2001

National Defence Défense nationale

Canada

A Novel Approach for the Wigner Distribution Formulation of the Optimum Detection Problem for a Discrete-Time Chirp Signal

T. Thayaparan
Defence Research Establishment Ottawa

A. Yasotharan
Unique Broadband System

Defence Research Establishment Ottawa

Technical Memorandum

DREO TM 2001-141

November 2001

Author

Thayananthan Thayaparan

Approved by

Maria Rey
Head, Surface Radar Section

Approved for release by

Gordon Marwood
Chief Scientist, Defence Research Establishment Ottawa

Abstract

The Wigner distribution is a signal transformation which has its origin in quantum mechanics. It possesses some important properties which make it very attractive for time-frequency signal analysis. The Wigner distribution was originally defined for continuous-time signals. A discrete-time version of it was proposed recently. Unfortunately, this discrete-time Wigner distribution suffers from aliasing effects, which prevent several of the properties of the continuous-time Wigner distribution from carrying over straightforwardly. In this report, a discrete-time Wigner distribution which does not suffer from aliasing is introduced. It is essentially an augmentation of the previous version, incorporating new information about the signal not contained in the previous version. A variety of methods have been proposed for the detection of a signal, with unknown signal parameters, in a noisy envirnoment. In this report, the noise statistics are incorporated to reveal that certain processing of the Wigner distribution signal representation can lead to an optimal, and often easy to compute, detection scheme. For the special case of discrete-time chirp signals in complex white Gaussian noise, it is shown that the optimal detector is equivalent to integrating the Wigner distribution along the line of instantaneous frequency. If the position and sweep rate of the linear chirp are unknown, then a Generalized Likelihood Ratio Test (GLRT) leads one to integrate the Wigner distribution along all possible lines in the time-frequency plane and choose the largest integrated value for comparison to a threshold. Simulation examples of the Wigner distribution scheme are given to demonstrate the utility concerning the detection of the proposed method.

Résumé

La distribution de Wigner est un outil de mise en forme de signal qui découle de la mécanique quantique. Elle possède certaines propriétés importantes qui en font un outil très intéressant pour l'analyse temps-fréquence des signaux. La distribution de Wigner a été définie à l'origine pour les signaux à temps continu. Une version à temps discret a été proposée récemment. Malheureusement, cette dernière présente des effets de repliement de spectre, de sorte que plusieurs des propriétés de la distribution de Wigner à temps continu ne peuvent lui être transférées directement. Dans le présent rapport, on traite d'une distribution de Wigner à temps discret qui ne comporte pas de repliement de spectre. Cette distribution consiste essentiellement en une extension de la version précédente, à laquelle ont été ajoutées de nouvelles données relatives au signal. Diverses méthodes ont été proposées pour la détection d'un signal, dont des paramètres sont inconnus, dans un environnement bruité. Dans le présent rapport, les statistiques sur le bruit sont incorporées afin de montrer que certains traitements de la représentation du signal sous forme d'une distribution de Wigner peuvent mener à un plan de détection optimal, comportant souvent des calculs relativement simples. Dans le cas particulier des impulsions modulées en fréquence à temps discret en présence de bruit blanc gaussien complexe, on montre que le détecteur optimal est obtenu en intégrant la distribution de Wigner suivant la ligne de fréquence instantanée. Si la position et la vitesse de balayage du signal à modulation de fréquence linéaire sont inconnues, un test généralisé du rapport des vraisemblances (TGRV) permet l'intégration de la distribution de Wigner suivant toutes les lignes possibles du plan temps-fréquence et la sélection de la plus grande valeur intégrée pour fins de comparaison à un seuil. Des exemples de simulation de plan de distribution de Wigner sont donnès dans le but de démontrer l'utilité en ce qui concerne la dètection de la mèthode proposée.

Executive summary

One of the central problems in High Frequency (HF) radar data is the analysis of a time series. The Fourier transform method, or Doppler processing method, has been generally used in HF radar to detect targets that are moving with constant radial acceleration. Examples of accelerating targets are manoeuvring aircrafts and missiles. Our previous studies show that there are limitations and shortcomings in the Fourier transform method to detect accelerating targets because of the phenomenon known as Doppler smearing [1,2]. Our studies also show that when the target is constantly accelerating, the Fourier method may still be used to detect the target and estimate its median velocity, provided the acceleration is small enough in the sense to be described in this report. It is shown that for a given acceleration, the number of pulses cannot be increased indefinitely without resulting in catastrophic failure of the method. Conversely, for a given number of pulses, the acceleration cannot be arbitrarily large without resulting in catastrophic failure of the method. Thus the number of pulses and the acceleration have to be matched to achieve optimum performance [1,2].

Consequently, for the interpretation of radar data in terms of a changing frequency content, we need a representation of our data as a function of both time and frequency. The purpose of this report is therefore to stress the importance of alternative methods which have been given little attention in the past, namely, the joint time-frequency representation of signals. In this report we choose the Wigner distribution together with a Radon transform as the basic tool, since both possess some important properties which are very attractive for time-frequency signal analysis [3].

A variety of methods have been proposed for the detection of a signal, with unknown signal parameters, in a noisy envirnoment. In this report, the noise statistics are incorporated to reveal that certain processing of the Wigner distribution signal representation can lead to an optimal, and often easy to compute, detection scheme. For the special case of discrete-time chirp signals in complex white Gaussian noise, it is shown that the optimal detector is equivalent to integrating the Wigner distribution along the line of instantaneous frequency. If the position and sweep rate of the linear chirp are unknown, then a Generalized Likelihood Ratio Test (GLRT) leads one to integrate the Wigner distribution along all possible lines in the time-frequency plane and choose the largest integrated value for comparison to a threshold. Simulation examples of the Wigner distribution scheme are given to demonstrate the utility concerning the detection of the proposed method.

In this report, a new discrete-time Wigner distribution has also been proposed. The ideas presented can be extented to formulate a Wigner distribution in both time and frequency, for discrete-time signals of finite duration, in the same spirit as development

of the discrete Fourier transform. Application of these ideas to actual data analysis is the subject of further research.

T. Thayaparan, A. Yasotharan. 2001. A Novel Approach for the Wigner Distribution Formulation of the Optimum Detection Problem for a Discrete-Time Chirp Signal. DREO TM 2001-141. Defence Research Establishment Ottawa.

Sommaire

Un des principaux problèmes éprouvé avec les données de radar haute fréquence (HF) est l'analyse d'une série chronologique. La méthode à transformée de Fourier, ou la méthode de traitement Doppler, a généralement été utilisée dans le radar HF pour la détection des cibles à accélération radiale constante. Les cibles présentant une accélération sont, par exemple, les aéronefs qui effectuent des manuvres et les missiles. Nos eétudes preéceédantes montre que la méthode à transformée de Fourier comporte des limites et des lacunes pour la détection des cibles à accélération, en raison du phénomène appelé la persistance Doppler [1,2]. Nos eétudes preéceédantes montre aussi que dans le cas d'une cible è accélération constante, la méthode de Fourier peut encore être appliquée pour détecter la cible et estimer sa vitesse médiane, à condition que l'accélération soit assez faible dans le contexte du présent rapport. On montre que pour une accélération donnée, le nombre d'impulsions ne peut pas être augmenté indéfiniment sans qu'il en résulte un échec catastrophique de la méthode. Inversement, pour un nombre donné d'impulsions, l'accélération ne peut pas augmenter arbitrairement sans qu'il en résulte aussi un échec catastrophique de la méthode. Ainsi, le nombre d'impulsions et l'accélération doivent être adaptés pour permettre des performances optimales [1,2].

Par conséquent, pour interpréter les données radar du point de vue d'un contenu en fréquences variable, nous devons les représenter aussi bien en fonction du temps qu'en fonction de la fréquence. L'objet du présent rapport est donc de souligner l'importance des méthodes de rechange auxquelles on a accordé peu d'attention par le passé, notamment la représentation temps-fréquence combinée des signaux. Dans le rapport, nous choisissons la distribution de Wigner avec une transformée de Radon comme outil de base, étant donné que ces deux éléments offrent certaines propriétés importantes qui présentent un grand intérêt pour l'analyse temps-fréquence des signaux [3].

Diverses méthodes ont été proposées pour la détection d'un signal, dont des paramètres sont inconnus, dans un environnement bruité. Dans le présent rapport, les statistiques sur le bruit sont incorporées afin de montrer que certains traitements de la représentation du signal sous forme d'une distribution de Wigner peuvent mener à un plan de détection optimal, comportant souvent des calculs relativement simples. Dans le cas particulier des impulsions modulées en fréquence à temps discret en présence de bruit blanc gaussien complexe, on montre que le détecteur optimal est obtenu en intégrant la distribution de Wigner suivant la ligne de fréquence instantanée. Si la position et la vitesse de balayage du signal à modulation de fréquence linéaire sont inconnues, un test généralisé du rapport des vraisemblances (TGRV) permet l'intégration de la distribution de Wigner suivant toutes les lignes possibles du plan temps-fréquence et la sélection de la plus grande valeur intégrée pour fins de comparaison à un seuil. Des exemples de simulation de plan de distribution de Wigner sont donnès dans le but de démontrer l'utilité en ce qui concerne la dètection de la mèthode proposée.

Dans le présent rapport, une nouvelle distribution de Wigner à temps discret a aussi été proposée. Les notions présentées peuvent être étendues à la formulation d'une distribution de Wigner tant dans le domaine temporel que dans le domaine fréquentiel, pour des signaux à temps discret de durée finie, dans le même esprit qui a été adopté pour l'élaboration de la transformée de Fourier discrète. L'application de ces notions à l'analyse de données réelles fait l'objet de recherches plus approfondies.

T. Thayaparan, A. Yasotharan. 2001. Nouvelle approche pour la formulation de la distribution de Wigner du problème de détection optimale d'un signal à temps discret.
DREO TM 2001-141. Centre de Recherches pour la Défense Ottawa.

Table of contents

List of figures

1. Introduction

The Fourier Transform is at the heart of a wide range of techniques that are used in radar data analysis and processing. Mapping the data into the temporal frequency domain is an effective way of recording the data such that their global characteristics can be assessed. However, the change of frequency content with time is one of the main features we observe in HF radar data. Because of this change of frequency content with time, radar signals belong to the class of non-stationary signals.

One of the central problems in High Frequency (HF) radar data is the analysis of a time series. The Fourier transform method, or Doppler processing method, has been generally used in HF radar to detect targets that are moving with constant radial acceleration. Examples of accelerating targets are manoeuvring aircrafts and missiles. Our previous studies show that there are limitations and shortcomings in the Fourier transform method to detect accelerating targets because of the phenomenon known as Doppler smearing [1,2]. Our studies also show that when the target is constantly accelerating, the Fourier method may still be used to detect a target and estimate its median velocity, provided the acceleration is small enough in the sense to be described in this report. It is shown that for a given acceleration, the number of pulses cannot be increased indefinitely without resulting in catastrophic failure of the method. Conversely, for a given number of pulses, the acceleration cannot be arbitrarily large without resulting in catastrophic failure of the method. Thus the number of pulses and the acceleration have to be matched to achieve optimum performance [1,2].

Consequently, for the interpretation of radar data in terms of a changing frequency content, we need a representation of our data as a function of both time and frequency. The purpose of this report is therefore to stress the importance of alternative methods which have been given little attention in the past, namely, the joint time-frequency representation of signals. The problem of detecting accelerating targets was looked at from two computational viewpoints: 1) Correlator method, that is, de-chirping followed by Doppler processing, and 2) Time-Frequency methods. The correlator method, although computationally costly, is optimum (maximum-likelihood), and hence serves as a benchmark. Time-Frequency methods have been considered before in a study done by [4]. The time-frequency method proposed in [4] was based on the definition of a discrete-time Wigner distribution given in [5]. This method, while providing insights into the problem, has the following drawbacks: 1) it is sub-optimal, 2) its maximum unambiguous range of measurable velocities is half of that of the correlator method, or of the conventional Doppler processing method [1], 3) it relies on an exhaustive search of the time-frequency plane in much the same way as the correlator method relies on an exhaustive search of the velocity-acceleration plane, and hence could not be implemented in real-time.

In this report, we derived a discrete-time Wigner time-frequency distribution which overcomes drawbacks 1) and 2). This distribution was independently derived by one of

[1] applicable when the target is non-accelerating or mildly accelerating, see [1] for more details

the authors [1]. But it had already been derived by Chan [6] in an effort to solve the problem of aliasing. Nevertheless, the optimality properties of this discrete-time Wigner distribution for signal detection were not observed in [6]. Therefore, in the context of signal detection, this discrete-time Wigner distribution seems new.

The performance of this new method depends on the signal-to-noise ratio and the length of the observation interval in exactly the same way as the performance of the conventional Doppler processing method for non-accelerating targets depends on the signal-to-noise ratio and the length of the observation interval. Performance analyses of the conventional Doppler processing method for non-accelerating targets is available in the literature, for example [7]. Therefore, the performance of our new Wigner distribution based method has been automatically quantified. This new Wigner distribution has led to the conception of an algorithm, which although is not optimal, could be implemented in real-time and hence would overcome drawback 3). The work presented in this report was carried out as part of a collaborative research contract from DREO to Raytheon Canada [1].

In the following section we define the signal model on which the algorithms are based. Section 3 discusses the maximum-likelihood method and its implementation as a correlator or as dechirping followed by Doppler processing. Section 4 discusses three Wigner distribution based methods, one of which is shown to be equivalent to the maximum-likelihood method. Section 5 identifies an algorithm that has real-time feasibility for further study. Finally, general conclusions are summarized in Section 6.

2. Signal Model and Detection and Parameter Estimation Problems

In this study, the radar is assumed to be of the Pulse Doppler type, that is, it sends out a uniform train of RF pulses and phase-coherently receives their returns. It is also assumed that the receiver has pulse compression capability so that a pulse return from an isolated target can be represented by a single sample of the compressed pulse [2].

2.1 Single-Target Scenario

Suppose the radar sends out N pulses, one every T seconds, and there is a target moving with constant radial acceleration. Assume that the range walk is negligible, that is, the change in range during the obeservation period of NT seconds is negligible compared to the radar range resolution as determined by the width of the compressed pulse. Then the samples of the N range-compressed pulses taken at the range of the targe have the form

$$r(n) = s(n) + v(n), \qquad \text{for } n = 0, 1, 2, 3, \ldots, (N-1), \tag{1}$$

where

$$s(n) = ae^{j(b_0 + b_1 n + \frac{1}{2} b_2 n^2)}, \tag{2}$$

is the noise-free signal, and $v(n)$ is a sequence of independently and identically distributed samples of complex Gaussian noise with zero mean and variance σ^2.

The signal parameters a and b_0 are the target amplitude and phase respectively. The signal parameters b_1 and b_2 are the normalized initial radial velocity and the normalized radial acceleration respectively.

2.1.1 Normalized Initial Velocity and Acceleration

The normalized initial radial velocity is defined as

$$b_1 = u\left(\frac{4\pi T}{\lambda}\right) \tag{3}$$

where u is the initial radial velocity in meters/sec, T is pulse repetition interval in secs, and λ is the carrier wavelength in meters. Similarly, the normalized radial acceleration is defined as

[2] Alternatively, the transmitted pulse may be narrow enough to achieve the same effect.

$$b_2 = f\left(\frac{4\pi T^2}{\lambda}\right) \tag{4}$$

where f is the radial acceleration in meters/sec/sec towards the radar. It can be seen that both of the above normalized quantities are non-dimensional.

To obtain these relations note that the increment in range d, measured from the beginning of the observation interval, as a function of continuous-time t, is $d(t) = ut + \frac{1}{2}ft^2$, and therefore the phase increment of a pulse as a function of discrete-time, or pulse index, is given by

$$2\pi\left(\frac{2d(nT)}{\lambda}\right) = \frac{4\pi}{\lambda}\left(unT + \frac{1}{2}fn^2T^2\right), \tag{5}$$

$$= u\left(\frac{4\pi T}{\lambda}\right)n + \frac{1}{2}f\left(\frac{4\pi T^2}{\lambda}\right)n^2. \tag{6}$$

In the rest of the discussion, the term *velocity* and *acceleration* refer to *normalized radial velocity* and *normalized radial acceleration* respectively.

2.1.2 Per-Pulse Signal-to-Noise Ratio

The Per-Pulse Signal-to-Noise Ratio is defined as

$$\mathrm{SNR}_{\mathrm{pulse}} = \left(\frac{a}{\sigma}\right)^2. \tag{7}$$

The performance measures of any detection method will depend on $\mathrm{SNR}_{\mathrm{pulse}}$ and the number of pulses N. The values of the signal parameters b_1 and b_2 may also influence performance. We are interested in detection methods whose performance will increase as N increases regardless of the values of b_1 and b_2.

2.2 Multiple-Target Scenario - Targets Separated in Range

When there are multiple targets, as long as they are separated from one another in range by at least the radar range resolution as determined by the width of the compressed pulse, a model of the above form will be valid for each of them.

Thus, if there are two targets separated in range, the samples of the N range-compressed pulses taken at the corresponding ranges of the targets have the form

(8) $r_1(n) = s_1(n) + v_1(n)$, and

(9) $r_2(n) = s_2(n) + v_2(n)$ for $n = 0, 1, 2, 3, \ldots, (N-1)$,

where $s_1(n)$ and $s_2(n)$ are the noise-free signals, and $v_1(n)$ and $v_2(n)$ are each sequences of independently and identically distributed (iid) samples of complex Gaussian noise with zero mean and variance σ^2.

Because of the independence of $v_1(n)$ and $v_2(n)$, the model decouples into two single target models.

2.3 Multiple-Target Scenario - Targets Coincident in Range

When there are multiple targets coincident in range, the samples of the N range-compressed pulses taken at the range of the targets have the form

(10) $r(n) = s(n) + v(n)$, for $n = 0, 1, 2, 3, \ldots, (N-1)$,

where $s(n)$ is the combined noise-free signal due to all targets and $v(n)$ is a sequence of independently and identically distributed (iid) samples of complex Gaussian noise with mean zero and variance σ^2. If there are K targets, the combined noise-free signal has the form

(11) $$s(n) = \sum_{k=1}^{K} a_k e^{j(b_{k,0} + b_{k,1} n + \frac{1}{2} b_{k,2} n^2)},$$

where a_k and $b_{k,0}$ are the amplitude and phase respectively of the k^{th} target, and $b_{k,1}$ and $b_{k,2}$ are the normalized initial radial velocity and the normalized radial acceleration respectively of the k^{th} target.

2.4 Target Amplitude and Phase Models

The target phase b_0 is assumed to be a random variable uniformly distributed over $[-\pi, \pi]$. The target amplitude a may be assumed to be a constant (Marcum, or Swerling-0) or a random variable [7]. Commonly assumed probability functions are the Rayleigh density (Swerling-1) and Rice density.

2.5 Detection Problem

Given the samples of the N range-compressed pulses taken at a particular range, the detection problem is to choose between the following hypotheses:

- Noise-only Hypothesis - $\mathbf{H_0}$, that is, the received signal $r(n)$ is due to noise alone,

$$r(n) = v(n), \tag{12}$$

- Signal-and-Noise Hypothesis - $\mathbf{H_1}$, that is, the received signal $r(n)$ is due to signal and noise,

$$r(n) = s(n) + v(n), \tag{13}$$

where the signal $s(n)$ may be due to the presence of one or more targets at the range of interest.

When there is more than one target, the 'Signal-and Noise' hypothesis can be subdivided on the basis of the number of hypothesized targets, or chirp signals, as '1 target and noise', '2 targets and noise', '3 targets and noise', and so on.

2.6 Parameter Estimation Problem

For the purpose of accurately tracking the accelerating targets we need to estimate their parameters, especially their kinematic parameters such as initial velocity, median velocity, and acceleration. Therefore, the problems of detecting the targets and estimating their parameters must be posed as a combined problem.

3. The Maximum Likelihood, or Generalized Likelihood Ratio Test, Method

In this section, the maximum likelihood, or generalized likelihood ratio test, method of detecting an accelerating target and estimating its parameters is described. This method is asymptotically optimum, and hence will sometimes be referred to as the optimum method in this report [8-12].

Recall from Section 2 that the detection problem is to choose between the Noise-Only Hypothesis - $\mathbf{H}_0$ and the Signal-and-Noise Hypothesis - $\mathbf{H}_1$.

Define

$$\Lambda(d, c_0, c_1, c_2) = \sum_{n=0}^{N-1} |r(n)|^2 - \sum_{n=0}^{N-1} \left| r(n) - d e^{j(c_0 + c_1 n + \frac{1}{2} c_2 n^2)} \right|^2. \tag{14}$$

Then

$$\max_{d, c_0, c_1, c_2} \Lambda(d, c_0, c_1, c_2) \underset{\mathbf{H}_0}{\overset{\mathbf{H}_1}{\gtrless}} \eta, \tag{15}$$

for some threshold η, is the maximum likelihood (ML), or generalized likelihood ratio test (GLRT), method. The maximizing values of d, c_0, c_1, and c_2 are the maximum likelihood estimates of a, b_0, b_1, and b_2 (see Section 2).

It can be shown that the above test can take the equivalent form

$$\max_{c_1, c_2} \Delta(c_1, c_2) \underset{\mathbf{H}_0}{\overset{\mathbf{H}_1}{\gtrless}} \gamma, \tag{16}$$

where

$$\Delta(c_1, c_2) = \left| \sum_{n=0}^{N-1} r(n) e^{-j(c_1 n + \frac{1}{2} c_2 n^2)} \right|^2, \tag{17}$$

and γ is a threshold (which can be related to η). Here the maximizing values of c_1 and c_2 are the maximum likelihood estimates of b_1 and b_2 respectively [1]. The optimum d and c_0 are given in terms of the optimum c_1 and c_2 by [1]

$$de^{jc_0} = \frac{1}{N}\sum_{n=0}^{N-1} r(n)e^{-j(c_1 n + \frac{1}{2}c_2 n^2)}. \tag{18}$$

Thus the ML, or GLRT, method can be implemented as a correlator in the initial velocity - acceleration plane. This method is also known as the dechirp-Doppler method, i.e., first multiplying by $e^{-j\frac{1}{2}c_2 n^2}$ to obtain a pure complex exponential, or nearly so, so that there will be little or no loss due to Doppler spreading when estimating the frequency of the pure complex exponential by the conventional Doppler processing method.

The notion of output SNR of the method comes from the observation that under the 'noise-only' hypothesis $\frac{2}{N\sigma^2}\Delta(c_1, c_2)$ is a central Chi-Squared random variable of two degrees of freedom, for all c_1 and c_2, whereas under the 'signal-and-noise' hypothesis, $\frac{2}{N\sigma^2}\Delta(b_1, b_2)$ is a non-central Chi-Squared random variable of two degrees of freedom and non-centrality parameter $2N\left(\frac{a}{\sigma}\right)^2$ [6,7].

We, therefore, consider

$$\mathrm{SNR}_{\mathrm{out}} = N\left(\frac{a}{\sigma}\right)^2. \tag{19}$$

as this can be used to approximately compute the probability of detcetion, which is sometimes assuming that the maximum of $\Delta(c_1, c_2)$ occurs at $c_1 = b_1$ and $c_2 = b_2$. Note that $\mathrm{SNR}_{\mathrm{out}}$ is a monotonically increasing function of N, but more specifically, it is a linearly increasing function of N.

3.1 The Cost of Computation for an Exhaustive Search

The cost of computing $\Delta(c_1, c_2)$, by brute-force, over K values of c_2 and M values of c_1 is

$$KM\mathcal{O}(N). \tag{20}$$

It is clear that for a given c_2, we can compute $\Delta(c_1, c_2)$ for M uniformly spaced discrete values of c_1 in the range $[-\pi, \pi]$ by using the FFT algorithm, provided $M \geq N$. Thus, if we desire to calculate $\Delta(c_1, c_2)$ over K values of c_2 and M values of c_1, uniformly spaced over $[-\pi, \pi]$ then the computational cost is

(21) $$KO(M \log M).$$

4. A Wigner-Distribution Formulation of the Optimum Detection Problem for a Discrete-Time Chirp Signal

In this section we formulate the maximum-likelihood, or optimum, detection of a discrete-time chirp signal in additive white Gaussian noise in terms of a Wigner distribution of the received signal $r(n)$. We do this by showing that $\Delta_r(c_1, c_2)$ can be interpreted as the integral along a straight line on the time-frequency plane of an appropriately defined Wigner distribution of the discrete-time signal $r(n)$.

Thus the maximization over c_1 and c_2 is transformed into maximization over straight lines whose intercept and slope parameters correspond to c_1 and c_2 respectively. At first this does not seem to offer any advantages over direct maximization of $\Delta_r(c_1, c_2)$. However, the Wigner distribution may suggest non-exhaustive, fast methods of searching and identifying the region in the time-frequency plane where the target's signal exists. This is especially so because, in the absence of noise or any other interference, the Wigner distribution of a discrete-time chirp signal is concentrated on a straight line of the time-frequency plane. A method based on this observation is identified in Section 5 for further investigation.

In the presence of interference of kinds other than white Gaussian noise, the Wigner distribution may suggest sub-optimal, robust methods of detection. For example, if some unwanted interference is known to be concentrated in a certain region of the time-frequency plane, then that interference can be filtered out and a cleaner signal can be synthesized for further processing by more conventional means.

4.1 Three Definitions of Wigner Distribution for Discrete-Time Signals

Given a discrete-time signal $r(n)$, we consider three definitions of auto time-frequency distributions which have some properties analogous to those of the classical Wigner distribution defined for continuous-time signals [13].

It is straightforward to verify that these are real-valued functions.

4.1.1 Type-I Wigner Distribution

The type-I Wigner distribution $W_r^I(n, \theta)$ is defined as

$$W_r^I(n, \theta) = \sum_k r(n+k) r^*(n-k) e^{-j2k\theta}, \tag{22}$$

where n is integer-valued and θ is real-valued. Note that this is the same as the definition provided in [5] except for the missing scaling factor 2 at the front.

It is easy to verify that the type-I Wigner distribution is a periodic function of θ with period π. This property will be discussed more in the following subsections.

For a signal $r(n)$ that is zero outside $0 \leq n \leq (N-1)$, the type-I Wigner distribution is zero outside $0 \leq n \leq (N-1)$.

4.1.2 Type-II Wigner Distribution

The type-II Wigner distribution $W_r^{II}(n,\theta)$ is defined as

$$W_r^{II}(n,\theta) = \sum_k r(n+k+1)r^*(n-k)e^{-j(2k+1)\theta}, \tag{23}$$

where n is integer-valued and θ is real-valued [1].

It is easy to verify that the type-II Wigner distribution is a periodic function of θ with period 2π. It is also easy to verify that

$$W_r^{II}(n,\theta+\pi) = -W_r^{II}(n,\theta). \tag{24}$$

These properties will be discussed more in the following subsections.

For a signal $r(n)$ that is zero outside $0 \leq n \leq (N-1)$, the type-II Wigner distribution is zero outside $0 \leq n \leq (N-2)$.

4.1.3 Type-III Wigner Distribution

The type-III Wigner distribution $W_r^{III}(n,\theta)$ is defined in terms of the type-I and type-II Wigner distributions as follows [1].

$$W_r^{III}(n,\theta) = \begin{cases} W_r^{I}(n/2,\theta) & \text{for even } n, \\ W_r^{II}((n-1)/2,\theta) & \text{for odd } n. \end{cases} \tag{25}$$

It is easy to verify that the type-III Wigner distribution is a periodic function of θ with period 2π. This property will be discussed more in in the following subsections.

For a signal $r(m)$ that is zero outside $0 \leq m \leq (N-1)$, the the type-III Wigner distribution is zero outside $0 \leq n \leq 2(N-1)$. However, if we consider even n to correspond to integer values of time and odd n to correspond to half-integer values of time then the type-III Wigner distribution is zero outside the time range $0 \leq m \leq (N-1)$.

4.2 Computing $\Delta_r(c_1, c_2)$ via the Wigner Distributions

In Appendix A we have shown that

$$\Delta_r(c_1, c_2) = \sum_{n=0}^{N-1} W_r^I(n, c_1 + c_2 n) + \sum_{n=0}^{N-2} W_r^{II}(n, c_1 + \frac{1}{2}c_2 + c_2 n), \tag{26}$$

$$\Delta_r(c_1, c_2) = \sum_{n=0}^{N-1} W_r^{III}(2n, c_1 + \frac{1}{2}c_2 2n) + \sum_{n=0}^{N-2} W_r^{III}(2n+1, c_1 + \frac{1}{2}c_2(2n+1)), \tag{27}$$

$$\Delta_r(c_1, c_2) = \sum_{n=0}^{2N-2} W_r^{III}(n, c_1 + \frac{1}{2}c_2 n). \tag{28}$$

Thus we can calculate $\Delta_r(c_1, c_2)$ by taking the type-III Wigner distribution $W_r^{III}(n, \theta)$ of the discrete-time received signal $r(n)$ and integrating it along the line with intercept c_1 (value of θ at $n = 0$) and slope $\frac{1}{2}c_2$ (increment in θ per unit increment in n).

This implies that we can perform optimum detection by the rule

$$\left(\max_{c_1, c_2} \sum_{n=0}^{2N-2} W_r^{III}(n, c_1 + \frac{1}{2}c_2 n) \right) \underset{\mathbf{H}_0}{\overset{\mathbf{H}_1}{\gtrless}} \gamma, \tag{29}$$

for some appropriately chosen threshold γ, where $\mathbf{H}_0$ and $\mathbf{H}_1$ are the 'noise only' and 'signal plus noise' hypotheses defined in Section 2.

The type-III Wigner distribution was independently derived by one of the authors [1]. But it had already been derived by Chan [6] in an effort to solve the problem of aliasing. Nevertheless, the optimality properties of this discrete-time Wigner distribution for signal detection were not observed in [6]. Therefore, in the context of signal detection, this discrete-time Wigner distribution seems new.

4.3 Three Definitions of Radon-Wigner Transform and Detection Methods Based on them for Discrete-Time Chirp Signals

Based on the results of Section 4.2, we can define the Radon-Wigner transform of a discrete-time signal in three ways and conceive of three detection methods for discrete-time chirp signals. In the literature the term 'Hough' transform is sometimes used to refer to what we have called 'Radon' transform. A more detailed description of the Radon transform can be found in [14].

4.3.1 Type-I Radon-Wigner transform and a detection method based on it

We shall refer to

$$RW_r^I(c_1, c_2) = \sum_{n=0}^{N-1} W_r^I(n, c_1 + c_2 n) \tag{30}$$

as the Type-I Radon-Wigner transform of $r(n)$ [1].

We may use the rule

$$\left(\max_{c_1, c_2} RW_r^I(c_1, c_2) \right) \underset{\mathbf{H_0}}{\overset{\mathbf{H_1}}{\gtrless}} \gamma^I, \tag{31}$$

for some appropriately chosen threshold γ^I, to detect discrete-time chirp signals.

Equation (30) can be summarized as follows. To optimally detect an accelerating target in white Guassian noise one should compute the wigner distribution of the observed data along all lines in the time-frequency plane. The maximum integrated value is then compared to a threshold and a detection is declared if the threshold is exceeded. It is interesting to note that this transformation of a signal via line integration to another 2-D signal is a Radon transform [14]. In practice, one usually has some a priori knowledge about the range of possible instantaneous frequency values which allows one to restrict the line integration to specific regions of the time-frequency plane.

4.3.2 Type-II Radon-Wigner transform and a detection method based on it

We shall refer to

$$RW_r^{II}(c_1, c_2) = \sum_{n=0}^{N-2} W_r^{II}(n, c_1 + \frac{1}{2}c_2 + c_2 n) \tag{32}$$

as the Type-II Radon-Wigner transform of $r(n)$ [1].

We may use the rule

$$\left(\max_{c_1, c_2} RW_r^{II}(c_1, c_2) \right) \underset{\mathbf{H}_0}{\overset{\mathbf{H}_1}{\gtrless}} \gamma^{II}, \tag{33}$$

for some appropriately chosen threshold γ^{II}, to detect discrete-time chirp signals.

4.3.3 Type-III Radon-Wigner transform and a detection method based on it

We shall refer to

$$RW_r^{III}(c_1, c_2) = \sum_{n=0}^{2N-2} W_r^{III}(n, c_1 + \frac{1}{2} c_2 n) \tag{34}$$

as the Type-III Radon-Wigner transform of $r(n)$ [1].

A rule based on this to detect discrete-time chirp signals has been stated in Section 3. We restate it as

$$\left(\max_{c_1, c_2} RW_r^{III}(c_1, c_2) \right) \underset{\mathbf{H}_0}{\overset{\mathbf{H}_1}{\gtrless}} \gamma. \tag{35}$$

4.3.4 A Common Error and its Consequences

It is a common error to assume

$$\Delta_r(c_1, c_2) = 2 \sum_{n=0}^{N-1} W_r^I(n, c_1 + c_2 n), \tag{36}$$

$$= 2RW_r^I(c_1, c_2), \tag{37}$$

and claim that optimum detection can be performed by the rule

$$\left(\max_{c_1, c_2} 2RW_r^I(c_1, c_2), \right) \underset{\mathbf{H}_0}{\overset{\mathbf{H}_1}{\gtrless}} \gamma. \tag{38}$$

This error was made in [4]. An historical reason for how this may have happened is given in Appendix B.

This error has the following negative consequences:

- A 50% reduction in the range of velocities that can be unambiguously measured,
- A loss in the asymptotic performance as measured by the output signal-to-ratio relative to the optimum method.

4.3.5 The Range of Unambiguously Measurable Velocities of the Type-I and Type-III Wigner Distribution Based Methods

As was shown in Section 4.1.1, the period of the type-I Wigner distribution is π. Therefore the signals

$$ae^{j(b_0+b_1n+\frac{1}{2}b_2n^2)}, \text{ and} \tag{39}$$

$$ae^{j(\tilde{b}_0+(b_1+\pi)n+\frac{1}{2}b_2n^2)}, \tag{40}$$

will give rise to the same type-I Wigner distribution. In otherwords, if we detect, using the type-I Wigner distribution, the presence of a signal in the time-frequency plane with intercept and slope parameters c_1 and c_2 respectively, then we cannot resolve the ambiguity as to whether the physical signal was

$$ae^{j(c_0+c_1n+\frac{1}{2}c_2n^2)}, \text{ or} \tag{41}$$

$$ae^{j(c_0+(c_1+\pi)n+\frac{1}{2}c_2n^2)} \tag{42}$$

without external information.

In contrast, as was shown in Section 4.1.3, the period of the type-III Wigner distribution is 2π. Therefore the signals

(43) $$ae^{j(b_0+b_1n+\frac{1}{2}b_2n^2)}, \text{ and}$$

(44) $$ae^{j(\tilde{b}_0+(b_1+\pi)n+\frac{1}{2}b_2n^2)},$$

will give rise to different type-III Wigner distributions.

If we detect, using the type-III Wigner distribution, the presence of a signal in the time-frequency plane with intercept and slope parameters c_1 and c_2 respectively, then there is no ambiguity as to whether the physical signal was

(45) $$ae^{j(c_0+c_1n+\frac{1}{2}c_2n^2)}, \text{ or}$$

(46) $$ae^{j(c_0+(c_1+\pi)n+\frac{1}{2}c_2n^2)}.$$

But we would of course need external information to resolve the ambiguity as to whether the physical signal was

(47) $$ae^{j(c_0+c_1n+\frac{1}{2}c_2n^2)}, \text{ or}$$

(48) $$ae^{j(c_0+(c_1+2\pi)n+\frac{1}{2}c_2n^2)}.$$

4.3.6 The Output Signal-to-Noise Ratio of the Type-I and Type-III Wigner Distribution Based Methods

Owing to the equivalence shown in Section 4.2, the output Signal-to-Noise Ratio (SNR) of the type-III Wigner distribution based method is the same as that of the optimum maximum likelihood method described in Section 3. The peformance results on the latter is available in the literature.

It was claimed in [15] that the output Signal-to-Noise Ratio (SNR) of the type-I Wigner distribution based method was less by 3dB than that of the $N(\frac{a}{\sigma})^2$ (i.e., type-III Wigner distribution based method).

4.4 The Wigner Distributions of the Discrete-Time Chirp Signal

In view of the results of Section 4.2, it is of interest to derive the type-I, type-II, and type-III Wigner distributions for the discrete-time chirp signal

(49) $$s(n) = ae^{j(b_0+b_1n+\frac{1}{2}b_2n^2)}, \text{ for } n = 0, 1, \ldots, (N-1),$$

defined in Section 2. These derivations have been done in Appendix C assuming $a = 1$. The results stated here are obtained by scaling those derived in the appendix by a^2. Note that the Wigner distributions do not depend on b_0.

4.4.1 The Type-I Wigner Distribution of $s(n)$

The Type-I Wigner Distribution $W_s^I(n,\theta)$ of $s(n)$ is given by [1]

$$W_s^I(n,\theta) = a^2 \begin{cases} 2\min(n, N-1-n)+1 & \text{if } \theta = b_1 + b_2 n \bmod \pi, \\ \frac{\sin[(\theta-(b_1+b_2 n))(2\min(n,N-1-n)+1)]}{\sin[\theta-(b_1+b_2 n)]} & \text{otherwise.} \end{cases} \tag{50}$$

for $0 \le n \le (N-1)$, and it is zero outside this range.

In a 3-dimensional plot, it has a ridge along the lines given by

$$\theta = b_1 + b_2 n \bmod \pi. \tag{51}$$

The height of the ridge is given by

$$2\min(n, N-1-n)+1. \tag{52}$$

4.4.2 The Type-II Wigner distribution of $s(n)$

The Type-II Wigner Distribution $W_s^{II}(n,\theta)$ of $s(n)$ is given by [1]

$$W_s^{II}(n,\theta) = a^2 \begin{cases} 2\min(n, N-2-n)+2 & \text{if } \theta = b_1 + \frac{1}{2}b_2 + b_2 n \bmod 2\pi, \\ -(2\min(n, N-2-n)+2) & \text{if } \theta = \pi + b_1 + \frac{1}{2}b_2 + b_2 n \bmod 2\pi, \\ \frac{\sin\left[\left(\theta-(b_1+\frac{1}{2}b_2+b_2 n)\right)(2\min(n,N-2-n)+2)\right]}{\sin\left[\theta-(b_1+\frac{1}{2}b_2+b_2 n)\right]} & \text{otherwise.} \end{cases} \tag{53}$$

for $0 \le n \le (N-2)$, and it is zero outside this range.

In a 3-dimensional plot, it has a ridge along the lines given by [1]

$$\theta = b_1 + \frac{1}{2}b_2 + b_2 n \bmod 2\pi. \tag{54}$$

The height of the ridge is given by

$$2\min(n, N-2-n)+2. \tag{55}$$

In a 3-dimensional plot, it also has a valley along the lines given by

(56) $$\theta = \pi + b_1 + \frac{1}{2}b_2 + b_2 n \bmod \pi.$$

The depth of the valley is given by

(57) $$2\min(n, N-2-n) + 2.$$

4.4.3 The Type-III Wigner distribution of $s(n)$

The Type-III Wigner Distribution $W_s^{III}(n,\theta)$ of $s(n)$ is given by

$$W_s^{III}(n,\theta) = a^2 \begin{cases} 2\min(\frac{n}{2}, N-1-\frac{n}{2})+1 & \text{if } \theta = b_1 + \frac{1}{2}b_2 n \bmod 2\pi, \\ (-1)^n \left[2\min(\frac{n}{2}, N-1-\frac{n}{2})+1\right] & \text{if } \theta = \pi + b_1 + \frac{1}{2}b_2 n \bmod 2\pi, \\ \frac{\sin\left[(\theta-(b_1+\frac{1}{2}b_2 n))(2\min(\frac{n}{2}, N-1-\frac{n}{2})+1)\right]}{\sin\left[\theta-(b_1+\frac{1}{2}b_2 n)\right]} & \text{otherwise.} \end{cases}$$

(58)

for $0 \le n \le 2(N-1)$, and it is zero outside this range.

In a 3-dimensional plot, it has a ridge along the lines given by

(59) $$\theta = b_1 + \frac{1}{2}b_2 n \bmod 2\pi.$$

The height of the ridge is given by

(60) $$\min(n, 2(N-1)-n) + 1.$$

In a 3-dimensional plot, it also has an oscillatory structure along the lines give by

(61) $$\theta = \pi + b_1 + \frac{1}{2}b_2 n \bmod 2\pi.$$

The period of the oscillation is one unit and the amplitude of the oscillation is given by

(62) $$\min(n, 2(N-1)-n) + 1.$$

4.5 A Numerical Example

The example of a two-target scenario, observed with $N = 128$, described in Section 2, is studied here using the three types of Wigner distribution based methods. The normalized initial velocity and normalized acceleration for target 1 are 0 and 0, respectively. For the target 2, the normalized initial velocity and normalized acceleration are 1 and 0.01, respectively.

Figure 1 shows the contour plot for the type-I Wigner distribution of the noise-free signal whereas Figure 2 shows the surface plot of the noise-free signal. Note that the time-frequency of the accelerating target's Wigner distribution is concentrated along a linear segment in the time-frequency plane. This linear segment corresponds to the instantaneous frequency. Figure 3 shows the contour plot for the type-I Wigner distribution of the noisy signal and Figure 4 shows the corresponding surface plot. For the Wigner distribution plotted in Figures 3 and 4, the targets were contaminated with the random white Guasian noise, such that the SNR was 5 dB. It is apparent that the type-I Wigner distribution is a periodic function with period π. Figures 5 and 6 show the type-I Radon-Wigner transform of the noise-free signal showing target 1 and target 2, respectively. Figures 7 and 8 show the type-I Radon-Wigner transform of the noisy signal showing target 1 and target 2, respectively. The plots of the Wigner distriburion and Radon-Wigner transform show that an accelereting target can be detected as easily as a non-accelerating target.

Figure 9 shows the contour plot for the type-II Wigner distribution of the noise-free signal and Figure 10 shows the surface plot of the noise-free signal. Figure 11 shows the contour plot for the type-II Wigner distribution of the noisy signal whereas Figure 12 shows the corresponding surface plot. It is evident that the type-II Wigner distribution is a periodic function with period 2π and $W_r^{II}(n, \theta + \pi) = -W_r^{II}(n, \theta)$ (see Section 4.1.2). Figures 13 and 14 show the type-II Radon-Wigner transform of the noise-free signal showing target 1 and target 2, respectively. Figures 15 and 16 show the type-II Radon-Wigner transform of the noisy signal showing target 1 and target 2, respectively. The plots of the Wigner distribution and the Radon-Wigner transforms show that an accelerating target can be detected as easily as a non-accelerating target.

Figure 17 shows the contour plot for the type-III Wigner distribution of the noise-free signal and Figure 18 shows the contour plot for the type-III Wigner distribution of the noisy signal. It is apparent that the type-III Wigner distribution is a periodic function with period 2π and this property is discussed more in Section 4.3.4. Figures 19 and 20 show the type-III Radon-Wigner transform of the noise-free signal showing target 1 and target 2, respectively. Figures 21 and 22 show the type-III Radon-Wigner transform of the noisy signal showing target 1 and target 2, respectively. The plots of the Wigner distribution and the Radon-Wigner transforms show that an accelerating target can be detected as easily as a non-accelerating target.

4.6 Type-I Wigner Distribution and its Radon Transform

4.6.1 Wigner Distribution

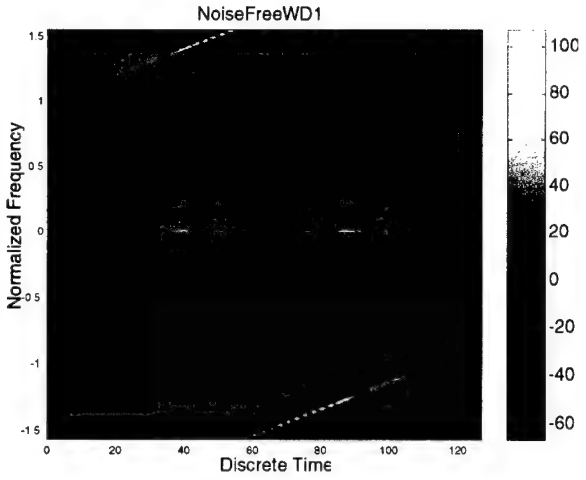

Figure 1: *The Type-I Wigner Distribution of the Noise-Free Signal.*

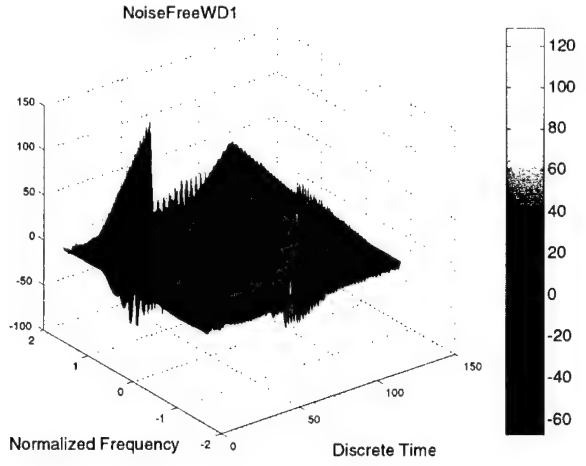

Figure 2: *The Type-I Wigner Distribution of the Noise-Free Signal.*

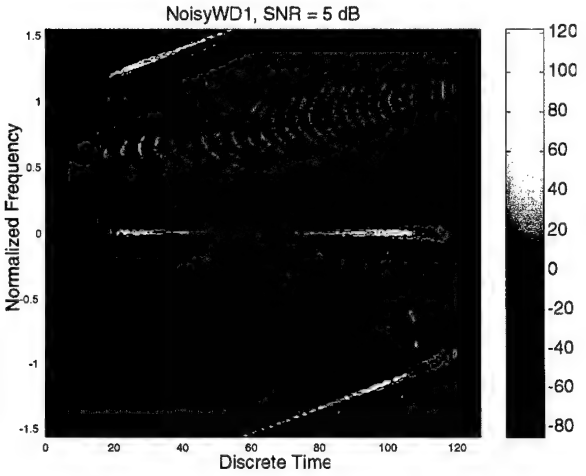

Figure 3: *The Type-I Wigner Distribution of the Noisy Signal.*

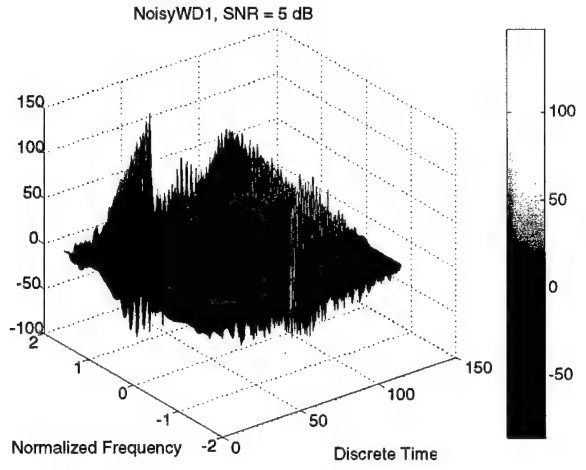

Figure 4: *The Type-I Wigner Distribution of the Noisy Signal.*

4.6.2 Radon Transform

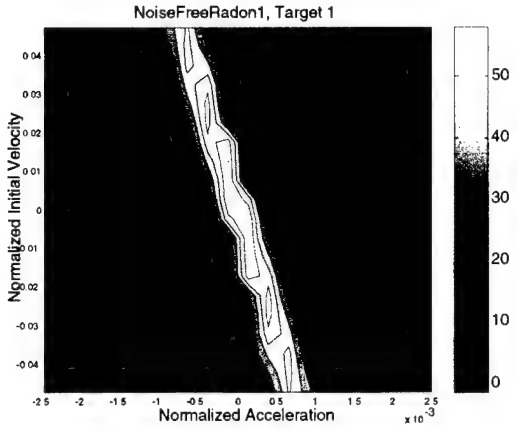

Figure 5: *The Type-I Radon-Wigner Transform of the Noise-Free Signal Showing Target 1.*

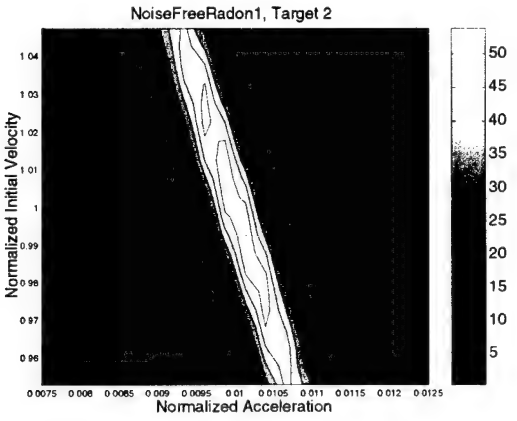

Figure 6: *The Type-I Radon-Wigner Transform of the Noise-Free Signal Showing Target 2.*

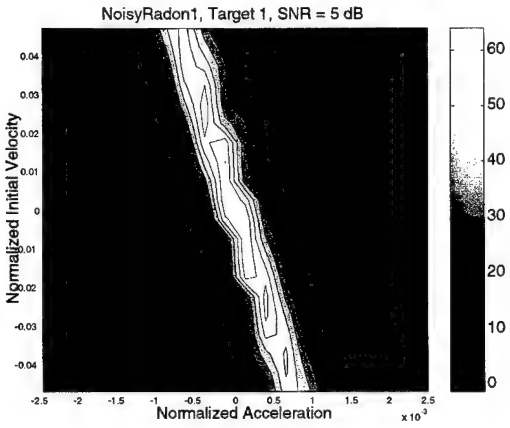

Figure 7: *The Type-I Radon-Wigner Transform of the Noisy Signal Showing Target 1.*

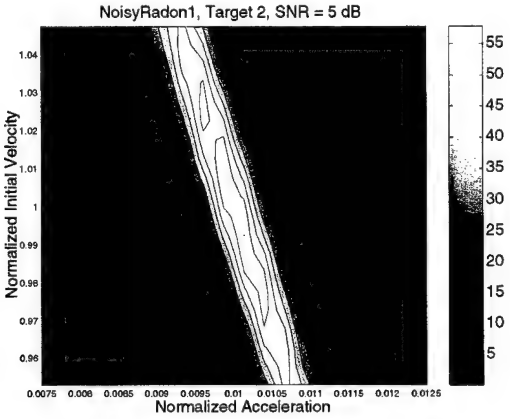

Figure 8: *The Type-I Radon-Wigner Transform of the Noisy Signal Showing Target 2.*

4.7 Type-II Wigner Distribution and its Radon Transform

4.7.1 Wigner Distribution

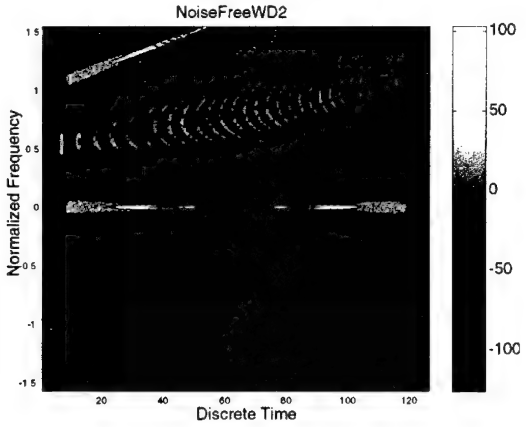

Figure 9: *The Type-II Wigner Distribution of the Noise-Free Signal.*

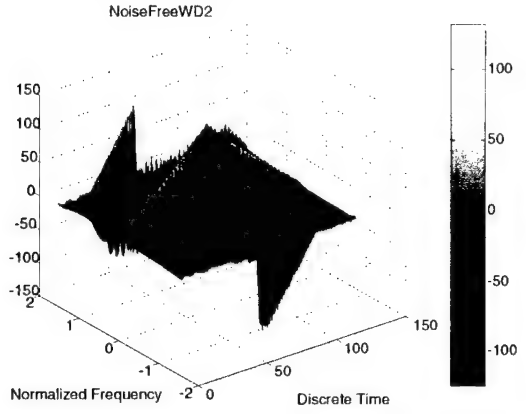

Figure 10: *The Type-II Wigner Distribution of the Noise-Free Signal.*

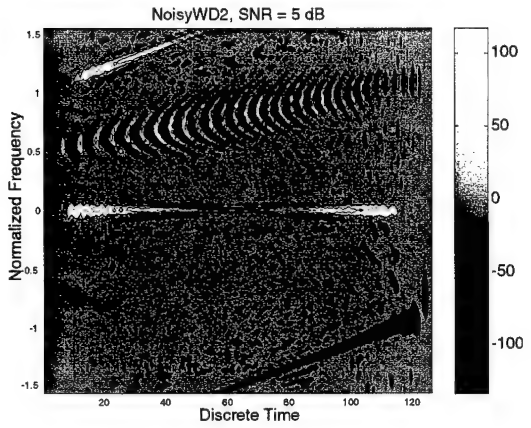

Figure 11: *The Type-II Wigner Distribution of the Noisy Signal.*

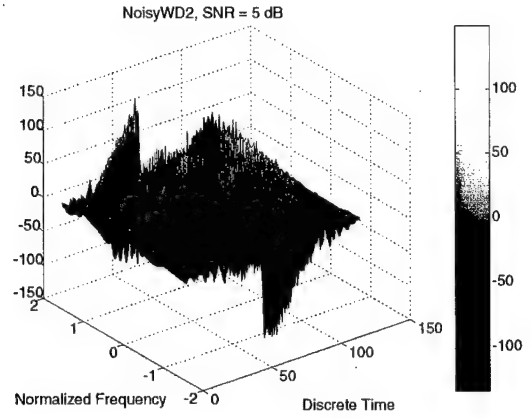

Figure 12: *The Type-II Wigner Distribution of the Noisy Signal.*

4.7.2 Radon Transform

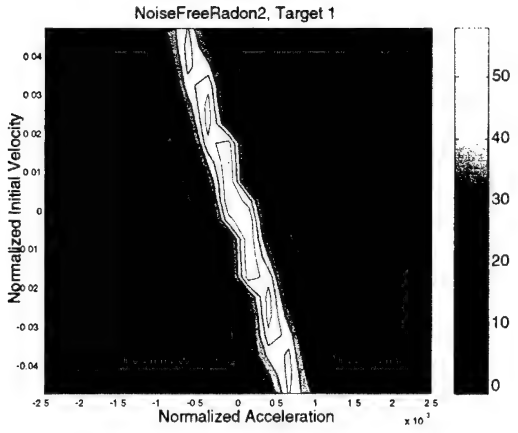

Figure 13: *The Type-II Radon-Wigner Transform of the Noise-Free Signal Showing Target 1.*

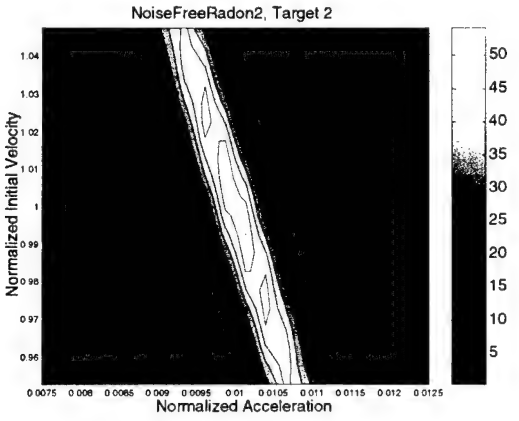

Figure 14: *The Type-II Radon-Wigner Transform of the Noise-Free Signal Showing Target 2.*

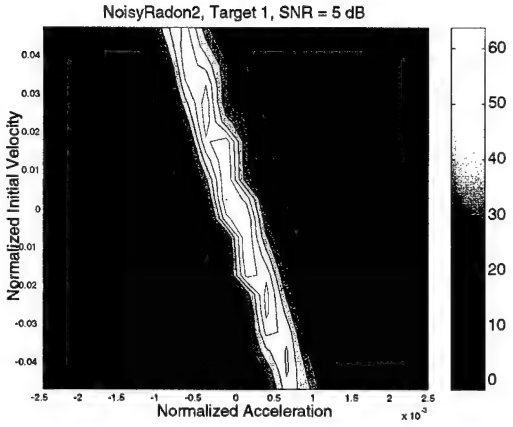

Figure 15: *The Type-II Radon-Wigner Transform of the Noisy Signal Showing Target 1.*

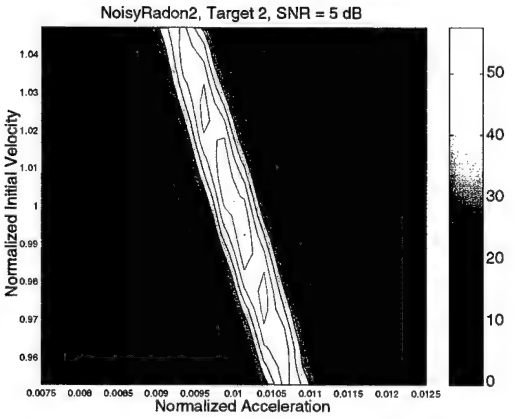

Figure 16: *The Type-II Radon-Wigner Transform of the Noisy Signal Showing Target 2.*

4.8 Type-III Wigner Distribution and its Radon Transform

4.8.1 Wigner Distribution

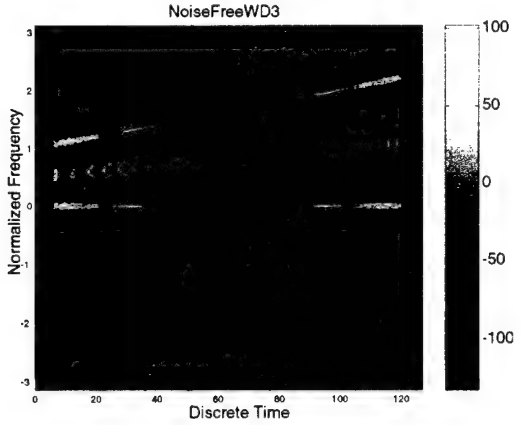

Figure 17: *The Type-III Wigner Distribution of the Noise-Free Signal.*

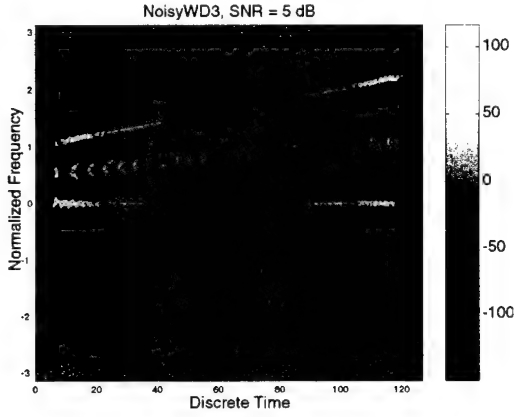

Figure 18: *The Type-III Wigner Distribution of the Noisy Signal.*

4.8.2 Radon Transform

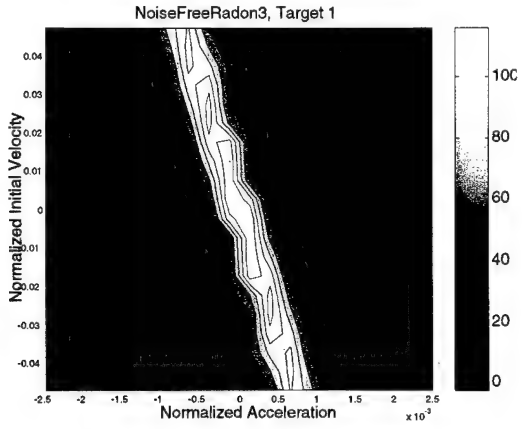

Figure 19: *The Type-III Radon-Wigner Transform of the Noise-Free Signal Showing Target 1.*

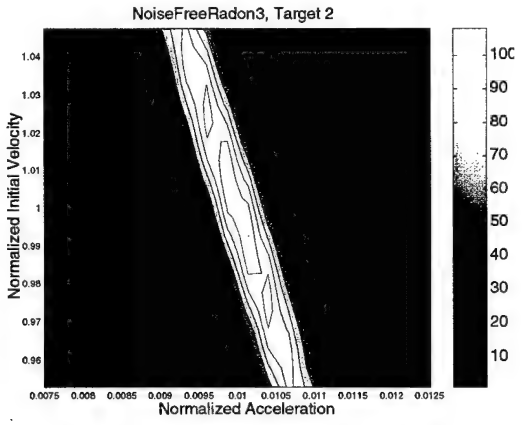

Figure 20: *The Type-III Radon-Wigner Transform of the Noise-Free Signal Showing Target 2.*

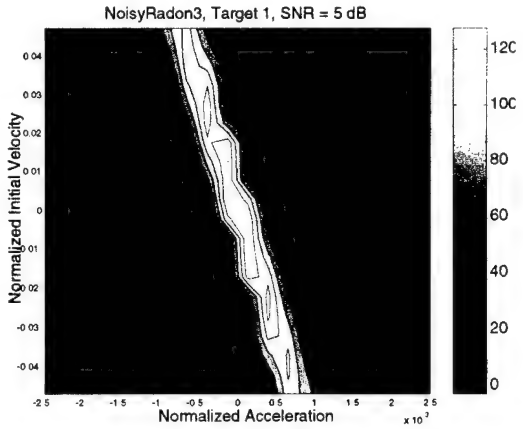

Figure 21: *The Type-III Radon-Wigner Transform of the Noisy Signal Showing Target 1.*

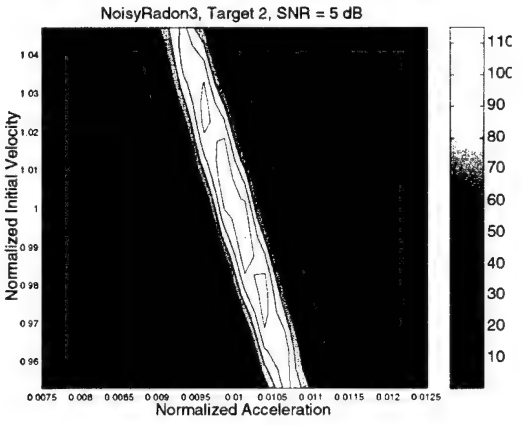

Figure 22: *The Type-III Radon-Wigner Transform of the Noisy Signal Showing Target 2.*

5. A Detection Method with Real-Time Feasibility

In this section a new method of detecting discrete-time chirp signals and estimating their parameters is described. It should be feasible to implement the method in real-time. Therefore, the method deserves further study.

This method is motivated by the type-II Wigner distribution defined in Section 4. More specifically, it makes use of the type-II Wigner distribution evaluated only at the center of the observation interval. The cost of computation can be shown to be of the order of that of a Fourier transform. We first consider detecting a single chirp signal. This will set the stage for considering the detection of multiple chirp signals.

5.1 Detecting a Single Chirp Signal

Recall from Appendix A that for the discrete-time chirp signal

$$s(n) = \begin{cases} e^{j(b_1 n + \frac{1}{2} b_2 n^2)} & \text{if } 0 \le n \le (N-1), \\ 0 & \text{otherwise,} \end{cases} \tag{63}$$

the type-II Wigner distribution is given for $0 \le n \le (N-2)$ by

$$W_s^{II}(n,\theta) = \begin{cases} 2\min(n, N-2-n)+2 & \text{if } \theta = b_1 + \frac{1}{2}b_2 + b_2 n \bmod 2\pi, \\ -(2\min(n, N-2-n)+2) & \text{if } \theta = \pi + b_1 + \frac{1}{2}b_2 + b_2 n \bmod 2\pi, \\ \frac{\sin\left[\left(\theta-(b_1+\frac{1}{2}b_2+b_2 n)\right)(2\min(n,N-2-n)+2)\right]}{\sin\left[\theta-(b_1+\frac{1}{2}b_2+b_2 n)\right]} & \text{otherwise.} \end{cases} \tag{64}$$

For a fixed n, the maximum of $W_s^{II}(n,\theta)$ with respect to θ occurs when

$$\theta = b_1 + \frac{1}{2}b_2 + b_2 n \bmod 2\pi. \tag{65}$$

Particularly, when N is even, for $n = \frac{N-2}{2}$, the maximum of $W_s^{II}(n,\theta)$ with respect to θ occurs when

$$\theta = b_1 + b_2\left(\frac{N-1}{2}\right) \bmod 2\pi. \tag{66}$$

Hereafter we shall assume that N is even. [3]

[3] For N odd we must consider the type-II Wigner distribution at either $n = \frac{N-3}{2}$ or $n = \frac{N-1}{2}$.

Therefore in the presence of noise, provided it is not too large, the chirp signal can be detected by the rule

$$\max_{\theta} W_r^{II}\left(\frac{N-2}{2},\theta\right) \underset{\mathbf{H}_0}{\overset{\mathbf{H}_1}{\gtrless}} \gamma_m, \tag{67}$$

for some appropriate γ_m, where $\mathbf{H}_1$ and $\mathbf{H}_0$ are the 'signal-plus-noise' and 'noise-only' hypotheses. If a signal is detected, then assuming that

$$\left|b_1 + b_2\left(\frac{N-1}{2}\right)\right| < \pi, \tag{68}$$

the maximizing θ, say c_m, can be taken as an estimate of the median frequency $b_m = b_1 + b_2\left(\frac{N-1}{2}\right)$ of the chirp signal over the observation interval $n = 0, \ldots, (N-1)$.

If an estimate of the frequency-rate b_2 is desired, it can be obtained by

$$\max_{\substack{c_1, c_2 \\ c_1 + c_2\left(\frac{N-1}{2}\right) = c_m}} \Delta_r(c_1, c_2), \tag{69}$$

that is by maximizing $\Delta_r(c_1, c_2)$ with respect to c_1 and c_2 under the constraint that $c_1 + c_2\left(\frac{N-1}{2}\right) = c_m$, where c_m is the estimate of the median frequency obtained based on $W_r^{II}(\frac{N-2}{2}, \theta)$ and

$$\Delta_r(c_1, c_2) = \left|\sum_{n=0}^{N-1} r(n) e^{-j(c_1 n + \frac{1}{2}c_2 n^2)}\right|^2. \tag{70}$$

We can restate the latter maximization problem as

$$\max_{c_2} \Delta_r\left(c_m - c_2\left(\frac{N-1}{2}\right), c_2\right). \tag{71}$$

For convenience we denote

$$\Gamma_r(c_m, c_2) = \Delta_r\left(c_m - c_2\left(\frac{N-1}{2}\right), c_2\right), \tag{72}$$

$$= \left|\sum_{n=0}^{N-1} r(n) e^{-j\left((c_m - c_2\left(\frac{N-1}{2}\right))n + \frac{1}{2}c_2 n^2\right)}\right|^2. \tag{73}$$

A better trade-off between the probabilities of 'miss' and 'false alarm' may be obtained by using a lower threshold γ_m in the first test and turning the second maximization problem into another test as[4]

$$\max_{c_2} \Gamma_r(c_m, c_2) \underset{\mathbf{H}_0}{\overset{\mathbf{H}_1}{\gtrless}} \gamma_a, \tag{74}$$

for some appropriate γ_a. This idea turns out to be useful for detecting multiple chirp signals.

5.2 Detecting Multiple Chirp Signals

The Wigner distribution of a superposition of signals contains cross terms, or interferences, between the signals. Suppose $s_1(n)$ and $s_2(n)$ are two signals, and $s(n) = s_1(n) + s_2(n)$. Then

$$W_s(n,\theta) = W_{s_1}(n,\theta) + W_{s_2}(n,\theta) + 2\Re\left(W_{s_1,s_2}(n,\theta)\right), \tag{75}$$

where $W_{s_1,s_2}(n,\theta)$ is the cross-Wigner distribution between $s_1(n)$ and $s_2(n)$. In time-frequency parlance, the terms $W_{s_1}(n,\theta)$ and $W_{s_2}(n,\theta)$ are called *auto*-terms and the term $2\Re\left(W_{s_1,s_2}(n,\theta)\right)$ is called a *cross*-term.

Suppose $s_1(n)$ and $s_2(n)$ are two discrete-time chirp signals, and consider the type-II Wigner distribution of $s(n) = s_1(n) + s_2(n)$. The large maxima of $W_s^{II}\left(\frac{N-2}{2}, \theta\right)$ with respect to θ will not all correspond to auto-terms; some of them will correspond to cross-terms. However, the auto-terms may be distinguished from the cross-terms as described below.

In the time-frequency plane, the auto-terms are localized to lines and the cross-terms are located half-way between the auto-terms. Although the cross-terms can be as large as the auto-terms, they exhibit an oscillatory behaviour in the direction of the line that

[4] When we do this, the meanings of $\mathbf{H}_0$ and $\mathbf{H}_1$ will change, but this is only of pedagogic significance.

is half-way between the lines to which the auto-terms are localized.[5] The auto-terms do not exhibit this oscillatory behaviour. Therefore, the auto-terms can be distinguished from the cross-terms by performing line-integrations in the time-frequency plane. Equivalently, we can perform correlations as described below.

Whether a maximum of $W_s^{II}\left(\frac{N-2}{2},\theta\right)$, at say $\theta = c_m$, corresponds to an auto-term or a cross-term can be decided by the rule

$$\max_{c_2} \Gamma_s(c_m, c_2) \underset{\mathbf{H}_{cross}}{\overset{\mathbf{H}_{auto}}{\gtrless}} \gamma_a, \tag{76}$$

for some appropriate γ_a, where $\mathbf{H}_{auto}$ and $\mathbf{H}_{cross}$ are the 'auto-term' and 'cross-term' hypotheses. If an auto-term is detected then the above maximization procedure will yield its frequency-rate parameter.

Therefore, in the presence of noise, multiple chirp signals can be detected by using the following two-stage procedure:

1. Identify all local maxima of $W_r^{II}\left(\frac{N-2}{2},\theta\right)$ with respect to θ that exceed γ_m,
2. For each local maxima identified in step 1, perform this test: Suppose $\theta = c_m$ is an identified local maximum, then maximize $\Gamma_r(c_m, c_2)$ with respect to c_2. If the maximum exceeds γ_a declare the presence of a chirp signal with median frequency c_m and frequency-rate c_2.

Note that this two-stage procedure is not different from the one described for detecting single chirp signals.

5.3 Further Enhancements

When considered as a function of θ, $W_s^{II}(\frac{N-2}{2},\theta)$ will have global maximum (main-lobe) at the median frequency and local maxima (side-lobes) on both sides. The ratio between the global maximum and the next largest local maximum, known as the peak sidelobe ratio, is about 13 dB. Thus a target can get masked by another target in its vicinity that is larger by 13 dB or more. To overcome this, we need to use some modified version of $W_s^{II}(\frac{N-2}{2},\theta)$ obtained by using a weighting function before taking the Fourier series sum.

The location of the cross-terms have a logical relation to the location of the auto-terms. A sophisticated method of distinguishing the cross-terms from the auto-terms that makes use of this information needs to be derived.

[5] The exact structure of a cross-term will be described later.

Time-frequency distributions that have the same periodicity properties as the type-II Wigner distribution but have reduced cross-terms need to be derived.

Having detected the real chirp signals and estimated their parameters, we can refine those estimates by using them as starting points for an iterative method of maximizing $\Delta_r(c_1, c_2)$. So, an iterative method of maximizing $\Delta_r(c_1, c_2)$ needs to be derived.

5.4 Cost of Computations Involved

Assuming we have some prior knowledge of the range of frequency-rates likely to be encountered, the cost is dominated by the cost of computing $W_r^{II}\left(\frac{N-2}{2}, \theta\right)$.

Recall from Section 4 that for N even

$$W_r^{II}\left(\frac{N-2}{2}, \theta\right) = \sum_{k=-N/2}^{N/2-1} r(N/2+k)r^*(N/2-1-k)e^{-j(2k+1)\theta}. \tag{77}$$

Obviously, this can be computed at M uniformly spaced values of θ over $[-\pi/2, \pi/2]$ in a straightforward way by using the Fast Fourier Transform algorithm provided $M \geq N$ and M is an integer power of 2. Denoting $a(k) = r(N/2+k)r^*(N/2-1-k)$, we see that $a(k) = a^*(-(k+1))$. This symmetry property allows us to reduce the cost roughly by a factor of two.

5.5 Consequences for Tracking

As was shown in Section 2, accelerating targets give rise to discrete-time chirp signals. Thus we can use the method described in this section to detect a constantly accelerating target and estimate its median velocity and acceleration.

As far as tracking a target is concerned, the availability of some form of velocity measurement should enhance the tracking performance over tracking based on range and azimuth measurements alone. A tracking algorithm for accelerating targets based on range, azimuth, and median radial velocity measurements should be easy to derive, especially if we have derived a tracking algorithm for non-accelerating targets based on range, azimuth, and radial velocity measurements. In the same vein, an implementation of a tracker for non-accelerating targets based on range, azimuth, and radial velocity measurements should be easily upgradable for tracking accelerating targets based on range, azimuth, and median radial velocity measurements.

To make use of the acceleration measurement, in addition to the median velocity measurement, an entirely new tracking algorithm needs to be derived.

6. Conclusion

A variety of methods have been proposed for the detection of a signal, with unknown signal parameters, in a noisy envirnoment. In this report, the noise statistics are incorporated to reveal that certain processing of the Wigner distribution signal representation can lead to an optimal, and often easy to compute, detection scheme. For the special case of linear FM signals in complex white Gaussian noise, it is shown that the optimal detector is equivalent to integrating the Wigner distribution along the line of instantaneous frequency. If the position and sweep rate of the linear chirp are unknown, then a Generalized Likelihood Ratio Test (GLRT) leads one to integrate the Wigner distribution along all possible lines in the time-frequency plane and choose the largest integrated value for comparison to a threshold. Simulation examples of the Wigner distribution scheme are given to demonstrate the utility concerning the detection of the proposed method.

In this report, a new discrete-time Wigner distribution has been also proposed. The ideas presented can be extented to formulate a Wigner distribution in both time and frequency, for discrete-time signals of finite duration, in the same spirit as development of discrete Fourier transform. Application of these ideas to actual data analysis is the subject of further research.

Annex A
Proof of Equation 5.3 of Section 2

Recall from Section 3 the definition

$$\Delta_r(c_1, c_2) = \left| \sum_{n=0}^{N-1} r(n) e^{-j(c_1 n + \frac{1}{2} c_2 n^2)} \right|^2 . \tag{A.1}$$

We can write this as the double summation

$$\Delta_r(c_1, c_2) = \sum_{n_1=0}^{N-1} \sum_{n_2=0}^{N-1} r(n_1) r^*(n_2) e^{-j(c_1(n_1-n_2) + \frac{1}{2} c_2 (n_1^2 - n_2^2))}, \tag{A.2}$$

$$= \sum_{n_1=0}^{N-1} \sum_{n_2=0}^{N-1} r(n_1) r^*(n_2) e^{-j(n_1-n_2)(c_1 + \frac{1}{2} c_2 (n_1+n_2))}. \tag{A.3}$$

Next we break the double summation into two double summations - one double summation being over n_1 and n_2 where $(n_1 - n_2)$ is even and the other double summation being over n_1 and n_2 where $(n_1 - n_2)$ is odd. Thus we define

$$\Delta_r^I(c_1, c_2) = \sum_{\substack{n_1=0 \\ (n_1-n_2) \text{ is even}}}^{N-1} \sum_{n_2=0}^{N-1} r(n_1) r^*(n_2) e^{-j(n_1-n_2)(c_1 + \frac{1}{2} c_2 (n_1+n_2))}, \tag{A.4}$$

and

$$\Delta_r^{II}(c_1, c_2) = \sum_{\substack{n_1=0 \\ (n_1-n_2) \text{ is odd}}}^{N-1} \sum_{n_2=0}^{N-1} r(n_1) r^*(n_2) e^{-j(n_1-n_2)(c_1 + \frac{1}{2} c_2 (n_1+n_2))}. \tag{A.5}$$

To compute $\Delta_r^I(c_1, c_2)$, we use the variable change [6]

$$n_1 + n_2 = 2m, \tag{A.6}$$

$$n_1 - n_2 = 2k, \tag{A.7}$$

[6] Note that $n_1 + n_2$ is even if and only if $n_1 - n_2$ is even for integers n_1, n_2.

and obtain

$$\Delta_r^I(c_1,c_2) = \sum_{m=0}^{N-1} \sum_{k=-\min(m,N-1-m)}^{\min(m,N-1-m)} r(m+k)r^*(m-k)e^{-j2k(c_1+c_2m)}, \tag{A.8}$$

$$= \sum_{m=0}^{N-1} W_r^I(m, c_1 + c_2 m) \tag{A.9}$$

$$= \sum_{m=0}^{N-1} W_r^I(m,\theta)\,|_{\theta=c_1+c_2m}. \tag{A.10}$$

Similarly, to compute $\Delta_r^{II}(c_1,c_2)$, we use the variable change

$$n_1 + n_2 = 2m + 1, \tag{A.11}$$

$$n_1 - n_2 = 2k + 1, \tag{A.12}$$

and obtain

$$\Delta_r^{II}(c_1,c_2) = \sum_{m=0}^{N-2} \sum_{k=-\min(m+1,N-1-m)}^{\min(m,N-2-m)} r(m+k+1)r^*(m-k)e^{-j(2k+1)(c_1+\frac{1}{2}c_2+c_2m)}, \tag{A.13}$$

$$= \sum_{m=0}^{N-2} W_r^{II}(m, c_1 + \frac{1}{2}c_2 + c_2 m) \tag{A.14}$$

$$= \sum_{m=0}^{N-2} W_r^{II}(m,\theta)\,|_{\theta=c_1+\frac{1}{2}c_2+c_2m}. \tag{A.15}$$

By combining these, we obtain

$$\Delta_r(c_1,c_2) = \Delta_r^I(c_1,c_2) + \Delta_r^{II}(c_1,c_2), \tag{A.16}$$

$$= \sum_{m=0}^{N-1} W_r^I(m, c_1 + c_2 m) + \sum_{m=0}^{N-2} W_r^{II}(m, c_1 + \frac{1}{2}c_2 + c_2 m), \tag{A.17}$$

$$= \sum_{m=0}^{N-1} W_r^{III}(2m, c_1 + \frac{1}{2}c_2 2m) + \sum_{m=0}^{N-2} W_r^{III}(2m+1, c_1 + \frac{1}{2}c_2(2m+1)),$$

(A.18)

$$= \sum_{\substack{m=0 \\ \text{(m is even)}}}^{2N-2} W_r^{III}(m, c_1 + \frac{1}{2}c_2 m) +$$

(A.19)

$$\sum_{\substack{m=0 \\ \text{(m is odd)}}}^{2N-2} W_r^{III}(m, c_1 + \frac{1}{2}c_2 m),$$

(A.20)

$$= \sum_{m=0}^{2N-2} W_r^{III}(m, c_1 + \frac{1}{2}c_2 m),$$

(A.21)

$$= \sum_{m=0}^{2N-2} W_r^{III}(m, \theta)\,|_{\theta = c_1 + \frac{1}{2}c_2 m}.$$

Thus we have proved equation (28) of section 4.2.

Annex B
A Historical Review of the Use of Wigner Distribution for Signal Detection

In this appendix, we provide a short historical review of the use of the Wigner distribution for signal detection in additive white Gaussian noise. This may explain how the error pointed out in Section 4.4.1 may have been committed.

B.1 The Case of Continuous-Time Signals

For a continous-time signal $r(t)$, the Wigner distribution is defined as [13]

$$W_r(t,\omega) = \int r(t+\tau/2)r^*(t-\tau/2)e^{-j\omega\tau}d\tau. \tag{B.1}$$

Suppose we have observed a continuous-time signal $r(t)$ and want to detect the presence or absence in $r(t)$ of a deterministic signal $s(t)$ with the backgorund being additive white Gaussian noise. The classical maximum-likelihood method can be based on the rule

$$\left|\int r(t)s^*(t)dt\right|^2 \underset{\mathbf{H_0}}{\overset{\mathbf{H_1}}{\gtrless}} \gamma, \tag{B.2}$$

where

- $\mathbf{H_0}$ is the Noise-Only Hypothesis - that is $r(t) = w(t)$,
- $\mathbf{H_1}$ is the Signal-plus-Noise Hypothesis - that is $r(t) = s(t) + w(t)$,

where $w(t)$ is white Gaussian noise. For the chirp signal

$$s(t) = e^{j(\omega_0 t + \frac{1}{2}mt^2)}, \tag{B.3}$$

the rule is

$$\left|\int r(t)e^{-j(\omega_0 t+\frac{1}{2}mt^2)}dt\right|^2 \underset{\mathbf{H_0}}{\overset{\mathbf{H_1}}{\gtrless}} \gamma. \tag{B.4}$$

In [12] the above rule was shown to be approximately equivalent to

$$\int_{-\infty}^{\infty} W_r(t, \omega_0 + mt) \underset{\mathbf{H_0}}{\overset{\mathbf{H_1}}{\gtrless}} \gamma \tag{B.5}$$

for chirp signals of large duration. The rule was rigourously shown to be valid even for chirp signals of finite duration in [16]. More Specifically it was shown in [16] that

$$\left| \int r(t) e^{-j(\omega_0 t + \frac{1}{2} m t^2)} dt \right|^2 = \int W_r(t, \omega_0 + mt) dt. \tag{B.6}$$

A more comprehensive study of the use of the time-frequency distributions for detecting signals is given by [17].

B.2 The Case of Discrete-Time Signals

For a discrete-time signal $r(n)$, the Wigner distribution defined by [5] has become widely accepted. Their definition of the Wigner distribution is

$$W_r^{CM}(n, \theta) = 2 \sum_k r(n+k) r^*(n-k) e^{-j2k\theta}, \tag{B.7}$$

which is twice the type-I Wigner distribution which we have provided in Section 4.1.1.

Suppose we have observed a discrete-time signal $r(n)$ and want to detect the presence or absence in $r(n)$ of a deterministic signal $s(n)$ with the background being additive white Gaussian noise. The classical maximum-likelihood method can be based on the rule

$$\left| \sum_n r(n) s^*(n) \right|^2 \underset{\mathbf{H_0}}{\overset{\mathbf{H_1}}{\gtrless}} \gamma, \tag{B.8}$$

where

- $\mathbf{H_0}$ is the Noise-Only Hypothesis - that is $r(n) = v(n)$,
- $\mathbf{H_1}$ is the Signal-plus-Noise Hypothesis - that is $r(n) = s(n) + v(n)$,

where $v(n)$ is white Gaussian noise. For the chirp signal

$$s(n) = e^{j(c_1 n + \frac{1}{2} c_2 n^2)}, \tag{B.9}$$

the rule is

$$\left| \sum_n r(n) e^{-j(c_1 n + \frac{1}{2} c_2 n^2)} \right|^2 \underset{\mathbf{H_0}}{\overset{\mathbf{H_1}}{\gtrless}} \gamma. \tag{B.10}$$

The equivalence of equation (104) for continuous-time signals was erroneously assumed to carry over to discrete-time signals as

$$\left| \sum_n r(n) e^{-j(c_1 n + \frac{1}{2} c_2 n^2)} \right|^2 = \sum_n W_r^{CM}(n, c_1 + c_2 n), \tag{B.11}$$

and it was claimed that maximum-likelihood detection can be based on the rule

$$\sum_n W_r^{CM}(n, c_1 + c_2 n) \underset{\mathbf{H_0}}{\overset{\mathbf{H_1}}{\gtrless}} \gamma. \tag{B.12}$$

Annex C
The Wigner Distributions of a Discrete-Time Chirp Signal

In this appendix we derive the type-I, type-II, and type-III Wigner distributions for the discrete-time chirp signal

$$s(n) = \begin{cases} e^{j(b_1 n + \frac{1}{2} b_2 n^2)} & \text{if } 0 \le n \le (N-1) \\ 0 & \text{otherwise.} \end{cases} \tag{C.1}$$

C.1 Type-I Wigner Distribution

Recall that the type-I Wigner distribution $W_s^I(n,\theta)$ is defined as

$$W_s^I(n,\theta) = \sum_k s(n+k)s^*(n-k)e^{-j2k\theta}, \tag{C.2}$$

where n is integer-valued and θ is real-valued.

It is easy to see that the signal product term $s(n+k)s^*(n-k)$ is zero outside the ranges $0 \le n \le (N-1)$ and $-\min(n, N-1-n) \le k \le \min(n, N-1-n)$. Thus $W_s^I(n,\theta) = 0$ outside $0 \le n \le (N-1)$.

Denote

$$l = \min(n, N-1-n) = \begin{cases} n & \text{if } n < (N-1)/2, \\ (N-1)/2 & \text{if } N \text{ is odd and } n = (N-1)/2, \\ N-1-n & \text{if } n > (N-1)/2. \end{cases} \tag{C.3}$$

In terms of this, for $0 \le n \le (N-1)$,

$$W_s^I(n,\theta) = \sum_{k=-l}^{l} e^{j(b_1(n+k)+\frac{1}{2}b_2(n+k)^2)} e^{-j(b_1(n-k)+\frac{1}{2}b_2(n-k)^2)} e^{-j2k\theta}, \tag{C.4}$$

$$= \sum_{k=-l}^{l} e^{j(b_1 2k + \frac{1}{2} b_2 4nk)} e^{-j2k\theta}, \tag{C.5}$$

$$= \sum_{k=-l}^{l} e^{-j(\theta-(b_1+b_2 n))2k}, \tag{C.6}$$

which is a sum of a geometric series that can be easily evaluated.

We first observe that the sum can be written as

$$\sum_{k=-l}^{l} e^{-j\alpha k}, \tag{C.7}$$

where $\alpha = 2(\theta - (b_1 + b_2 n))$ and then evaluate it to be

$$\sum_{k=-l}^{l} e^{-j\alpha k} = \begin{cases} 2l+1 & \text{if } \alpha = 0 \bmod 2\pi, \\ \frac{\sin\left[\alpha(l+\frac{1}{2})\right]}{\sin(\frac{\alpha}{2})} & \text{otherwise.} \end{cases} \tag{C.8}$$

Thus, for $0 \leq n \leq (N-1)$,

$$W_s^I(n,\theta) = \begin{cases} 2\min(n, N-1-n)+1 & \text{if } \theta = b_1 + b_2 n \bmod \pi, \\ \frac{\sin[(\theta-(b_1+b_2 n))(2\min(n,N-1-n)+1)]}{\sin[\theta-(b_1+b_2 n)]} & \text{otherwise.} \end{cases} \tag{C.9}$$

C.2 Type-II Wigner Distribution

Recall that the type-II Wigner distribution $W_s^{II}(n,\theta)$ is defined as

$$W_s^{II}(n,\theta) = \sum_k s(n+k+1)s^*(n-k)e^{-j(2k+1)\theta}, \tag{C.10}$$

where n is integer-valued and θ is real-valued.

It is easy to see that the signal product term $s(n+k+1)s^*(n-k)$ zero outside the ranges $0 \leq n \leq (N-2)$ and $-\min(n+1, N-1-n) \leq k \leq \min(n, N-2-n)$. Thus $W_s^{II}(n,\theta) = 0$ outside $0 \leq n \leq (N-2)$.

Denote

$$l = \min(n, N-2-n) = \begin{cases} n & \text{if } n < (N-2)/2, \\ (N-2)/2 & \text{if } N \text{ is even and } n = (N-2)/2, \\ N-2-n & \text{if } n > (N-2)/2. \end{cases} \tag{C.11}$$

In terms of this, for $0 \leq n \leq (N-2)$,

$$W_s^{II}(n,\theta) = \sum_{k=-(l+1)}^{l} e^{j(b_1(n+k+1)+\frac{1}{2}b_2(n+k+1)^2)} e^{-j(b_1(n-k)+\frac{1}{2}b_2(n-k)^2)} e^{-j(2k+1)\theta},$$

(C.12)

$$= \sum_{k=-(l+1)}^{l} e^{j(b_1(2k+1)+\frac{1}{2}b_2(4nk+2n+2k+1))} e^{-j(2k+1)\theta}, \quad \text{(C.13)}$$

$$= \sum_{k=-(l+1)}^{l} e^{-j(\theta-(b_1+\frac{1}{2}b_2+b_2n))(2k+1)}, \quad \text{(C.14)}$$

$$= e^{-j(\theta-(b_1+\frac{1}{2}b_2+b_2n))} \sum_{k=-(l+1)}^{l} e^{-j(\theta-(b_1+\frac{1}{2}b_2+b_2n))2k}, \quad \text{(C.15)}$$

which is a scaled version of a sum of a geometric series that can be easily evaluated.

We first observe that the sum can be written as

$$\sum_{k=-(l+1)}^{l} e^{-j\alpha k}, \quad \text{(C.16)}$$

where $\alpha = 2(\theta - (b_1 + \frac{1}{2}b_2 + b_2 n))$ and then evaluate it to be

$$\sum_{k=-(l+1)}^{l} e^{-j\alpha k} = \begin{cases} 2l+2 & \text{if } \alpha = 0 \bmod 2\pi, \\ e^{j\frac{\alpha}{2}} \left(\frac{\sin[\alpha(l+1)]}{\sin(\frac{\alpha}{2})} \right). \end{cases} \quad \text{(C.17)}$$

Now, introducing the scaling factor, we see that

$$e^{-j\frac{\alpha}{2}} \sum_{k=-(l+1)}^{l} e^{-j\alpha k} = \begin{cases} e^{-j\frac{\alpha}{2}}(2l+2) & \text{if } \alpha = 0 \bmod 2\pi, \\ \frac{\sin[\alpha(l+1)]}{\sin(\frac{\alpha}{2})}. \end{cases} \quad \text{(C.18)}$$

$$= \begin{cases} (2l+2) & \text{if } \frac{\alpha}{2} = 0 \bmod 2\pi, \\ -(2l+2) & \text{if } \frac{\alpha}{2} = \pi \bmod 2\pi, \\ \frac{\sin[\alpha(l+1)]}{\sin(\frac{\alpha}{2})}. \end{cases} \quad \text{(C.19)}$$

Thus, for $0 \leq n \leq (N-2)$,

$$W_s^{II}(n,\theta) = \begin{cases} 2\min(n, N-2-n)+2 & \text{if } \theta = b_1 + \frac{1}{2}b_2 + b_2 n \bmod 2\pi, \\ -(2\min(n, N-2-n)+2) & \text{if } \theta = \pi + b_1 + \frac{1}{2}b_2 + b_2 n \bmod 2\pi, \\ \frac{\sin\left[\left(\theta-(b_1+\frac{1}{2}b_2+b_2 n)\right)(2\min(n,N-2-n)+2)\right]}{\sin\left[\theta-(b_1+\frac{1}{2}b_2+b_2 n)\right]} & \text{otherwise.} \end{cases}$$

(C.20)

It is useful to write this as

$$W_s^{II}(n,\theta) = \begin{cases} 2\min(n+\frac{1}{2}, N-1-(n+\frac{1}{2}))+1 & \text{if } \theta = b_1 + b_2(n+\frac{1}{2}) \bmod 2\pi, \\ -\left[2\min(n+\frac{1}{2}, N-1-(n+\frac{1}{2}))+1\right] & \text{if } \theta = \pi + b_1 + b_2(n+\frac{1}{2}) \bmod 2\pi, \\ \frac{\sin\left[\left(\theta-(b_1+b_2(n+\frac{1}{2}))\right)\left(2\min(n+\frac{1}{2},N-1-(n+\frac{1}{2}))+1\right)\right]}{\sin\left[\theta-(b_1+b_2(n+\frac{1}{2}))\right]} & \text{otherwise.} \end{cases}$$

(C.21)

C.3 Type-III Wigner Distribution

Recall that the type-III Wigner distribution $W_s^{III}(n,\theta)$ is defined in terms of the type-I and type-II Wigner distributions as

$$W_s^{III}(n,\theta) = \begin{cases} W_s^I(n/2,\theta) & \text{for even } n, \\ W_s^{II}((n-1)/2,\theta) & \text{for odd } n. \end{cases} \tag{C.22}$$

For n even and $0 \le n \le 2(N-1)$,

$$W_s^{III}(n,\theta) = \begin{cases} 2\min(\frac{n}{2}, N-1-\frac{n}{2})+1 & \text{if } \theta = b_1 + \frac{1}{2}b_2 n \bmod \pi, \\ \frac{\sin\left[\left(\theta-(b_1+\frac{1}{2}b_2 n)\right)\left(2\min(\frac{n}{2},N-1-\frac{n}{2})+1\right)\right]}{\sin\left[\theta-(b_1+\frac{1}{2}b_2 n)\right]} & \text{otherwise.} \end{cases} \tag{C.23}$$

For n odd and $0 \le n \le 2(N-1)$,

$$W_s^{III}(n,\theta) = \begin{cases} 2\min(\frac{n}{2}, N-1-\frac{n}{2})+1 & \text{if } \theta = b_1 + \frac{1}{2}b_2 n \bmod 2\pi, \\ -\left[2\min(\frac{n}{2}, N-1-\frac{n}{2})+1\right] & \text{if } \theta = \pi + b_1 + \frac{1}{2}b_2 n \bmod 2\pi, \\ \frac{\sin\left[\left(\theta-(b_1+\frac{1}{2}b_2 n)\right)\left(2\min(\frac{n}{2},N-1-\frac{n}{2})+1\right)\right]}{\sin\left[\theta-(b_1+\frac{1}{2}b_2 n)\right]} & \text{otherwise.} \end{cases}$$

(C.24)

Combining the above, for all $0 \le n \le 2(N-1)$,

$$W_s^{III}(n,\theta) = \begin{cases} 2\min(\frac{n}{2}, N-1-\frac{n}{2})+1 & \text{if } \theta = b_1 + \frac{1}{2}b_2 n \bmod 2\pi, \\ (-1)^n \left[2\min(\frac{n}{2}, N-1-\frac{n}{2})+1\right] & \text{if } \theta = \pi + b_1 + \frac{1}{2}b_2 n \bmod 2\pi, \\ \frac{\sin\left[\left(\theta-(b_1+\frac{1}{2}b_2 n)\right)\left(2\min(\frac{n}{2}, N-1-\frac{n}{2})+1\right)\right]}{\sin\left[\theta-(b_1+\frac{1}{2}b_2 n)\right]} & \text{otherwise.} \end{cases}$$

(C.25)

Acknowledgment

The work was carried out as part of a collaborative research contract from Defence Research Establihsment Ottawa to Raytheon Canada (DREO Ref. W7714-8-0183/001/SV, RSCL Ref. DND339).

References

1. Yasotharan, A. (1999). On detecting and tracking accelerating targets by a pulse Doppler radar - final report on phase 1 of contract with DREO, Contract W7714-8-0183/001/Sv, Raytheon Canada Limited.

2. Thayaparan, T. and Yasotharan, A. (2000). Limitations and Strengths of the Fourier transform method to detect accelerating targets. Defence Research Establishment Ottawa, *DREO TM 2000-078.*

3. Thayaparan, T. (2000). Linear and Quadratic time-frequency representations. Defence Research Establishment Ottawa, *DREO TM 2000-080.*

4. Raytheon Canada Limited. (1996). Development of Time Frequency Techniques for Missile Detection. Report Prepared for DREO under contract W7714-5-9922/001-SL.

5. Claasen, T. A. C. M. and Mecklenbrauker, W. F. G. (1980). The Wigner Distribution - A Tool for Time-Frequency Signal Analysis, Part-II: Discrete-Time Signals. *Philips Journal of Research,* Vol. 35, Nos. 4/5, 276-300.

6. Chan, D. S. K. (1982). A Non-Aliased Discrete-Time Wigner Distribution for Time-Frequency Signal Analysis. *Proc. ICASSP '82,* 1333-1336.

7. Meyer, D. P. and Mayer, H. A. (1973). Radar Target Detection - Handbook of Theory and Practice. *Academic Press,* New York, USA.

8. Whalen, A. D. (1971). Detection of signals in noise. *Academic press,* New York, USA.

9. Kendall, M. and Stuart, A. (1979). The advanced theory of statistics Vol. II. *Macmillan Publishing Co.,* New York, USA.

10. Kay, S. M. (1993). Foundamentals of statistical signal processing - detection theory *Prentice hall PTR,* New Jersey, USA.

11. Abatzoglou, T. J. (1986). Fast Maximum Likelihood Joint Estimation of Frequency and Frequency Rate *IEEE Trans. Aerospace and Electronic Systems,* Vol. AES-22, No. 6, 708- 715.

12. Kay, S. and Boudreaux-Bartels, G. F. (1985). On the Optimality of the Wigner Distribution for Detection, *Proc. ICASSP '85,* 27.2.1-4.

13. Claasen, T. A. C. M. and Mecklenbrauker, W. F. G. (1980). The Wigner Distribution - A Tool for Time-Frequency Signal Analysis, Part-I: Continuous-Time Signals. *Philips Journal of Research,* Vol. 35, No. 3, 217-250.

14. Rattey, P. A. and Lindgren, A. G. (1981). Sampling the 2-D transform. *IEEE Trans. ASSP,* vol. ASSP-29, No. 9 994-1002, October.

15. Barbarossa, S. (1995). Analysis of Multicomponent LFM Signals by a Combined Wigner-Hough Transform. *IEEE Trans. Signal Processing,* Vol. 43, No. 6, 1511-1515, June.

16. Li, W. (1987). Wigner Distribution Method Equivalent to Dechirp Method for Detecting a Chirp Signal *IEEE Trans. Acoustics, Speech, and Signal Processing,* Vol. ASSP-35, No. 8, 1210-1211, August.

17. Flandrin, P. (1988). A Time-Frequency Formulation of Optimum Detection. *IEEE Trans. Acoustics, Speech, and Signal Processing,* Vol. 36, No. 9, 1377-1384, September.

DOCUMENT CONTROL DATA

(Security classification of title, body of abstract and indexing annotation must be entered when the overall document is classified)

1. ORIGINATOR (the name and address of the organization preparing the document. Organizations for whom the document was prepared, e.g. Establishment sponsoring a contractor's report, or tasking agency, are entered in section 8.)

Defence Research Establishment Ottawa
Department of National Defence
Ottawa, Ontario, Canada K1A 0Z4

2. SECURITY CLASSIFICATION (overall security classification of the document, including special warning terms if applicable)

UNCLASSIFIED

3. TITLE (the complete document title as indicated on the title page. Its classification should be indicated by the appropriate abbreviation (S,C or U) in parentheses after the title.)

A Novel Approach for the Wigner Distribution Formulation of the Optimum Detection Problem for a Discrete-Time Signal (U)

4. AUTHORS (Last name, first name, middle initial)

Thayaparan, Thayananthan and Yasotharan, Ambighairajah

5. DATE OF PUBLICATION (month and year of publication of document)

November 2001

6a. NO. OF PAGES (total containing information. Include Annexes, Appendices, etc.)

50

6b. NO. OF REFS (total cited in document)

17

7. DESCRIPTIVE NOTES (the category of the document, e.g. technical report, technical note or memorandum. If appropriate, enter the type of report, e.g. interim, progress, summary, annual or final. Give the inclusive dates when a specific reporting period is covered.)

DREO TECHNICAL MEMORANDUM

8. SPONSORING ACTIVITY (the name of the department project office or laboratory sponsoring the research and development. Include the address.)

Defence Research Establishment Ottawa
Department of National Defence
Ottawa, Ontario, Canada K1A 0Z4

9a. PROJECT OR GRANT NO. (if appropriate, the applicable research and development project or grant number under which the document was written. Please specify whether project or grant)

05AB11

9b. CONTRACT NO. (if appropriate, the applicable number under which the document was written)

10a. ORIGINATOR'S DOCUMENT NUMBER (the official document number by which the document is identified by the originating activity. This number must be unique to this document.)

DREO TM 2001-141

10b. OTHER DOCUMENT NOS. (Any other numbers which may be assigned this document either by the originator or by the sponsor)

11. DOCUMENT AVAILABILITY (any limitations on further dissemination of the document, other than those imposed by security classification)

(X) Unlimited distribution
( ) Distribution limited to defence departments and defence contractors; further distribution only as approved
( ) Distribution limited to defence departments and Canadian defence contractors; further distribution only as approved
( ) Distribution limited to government departments and agencies; further distribution only as approved
( ) Distribution limited to defence departments; further distribution only as approved
( ) Other (please specify):

12. DOCUMENT ANNOUNCEMENT (any limitation to the bibliographic announcement of this document. This will normally correspond to the Document Availability (11). However, where further distribution (beyond the audience specified in 11) is possible, a wider announcement audience may be selected.)

13. ABSTRACT (a brief and factual summary of the document. It may also appear elsewhere in the body of the document itself. It is highly desirable that the abstract of classified documents be unclassified. Each paragraph of the abstract shall begin with an indication of the security classification of the information in the paragraph (unless the document itself is unclassified) represented as (S), (C), or (U). It is not necessary to include here abstracts in both official languages unless the text is bilingual).

(U) The Wigner distribution is a signal transformation which has its origin in quantum mechanics. It possesses some important properties which make it very attractive for time-frequency signal analysis. The Wigner distribution was originally defined for continuous-time signals. A discrete-time version of it was proposed recently. Unfortunately, this discrete-time Wigner distribution suffers from aliasing effects, which prevent several of the properties of the continuous-time Wigner distribution from carrying over straightforwardly. In this report, a discrete-time Wigner distribution which does not suffer from aliasing is introduced. It is essentially an augmentation of the previous version, incorporating new information about the signal not contained in the previous version. A variety of methods have been proposed for the detection of a signal, with unknown signal parameters, in a noisy envirnoment. In this report, the noise statistics are incorporated to reveal that certain processing of the Wigner distribution signal representation can lead to an optimal, and often easy to compute, detection scheme. For the special case of discrete-time chirp signals in complex white Gaussian noise, it is shown that the optimal detector is equivalent to integrating the Wigner distribution along the line of instantaneous frequency. If the position and sweep rate of the linear chirp are unknown, then a Generalized Likelihood Ratio Test (GLRT) leads one to integrate the Wigner distribution along all possible lines in the time-frequency plane and choose the largest integrated value for comparison to a threshold. Simulation examples of the Wigner distribution scheme are given to demonstrate the utility concerning the detection of the proposed method.

14. KEYWORDS, DESCRIPTORS or IDENTIFIERS (technically meaningful terms or short phrases that characterize a document and could be helpful in cataloguing the document. They should be selected so that no security classification is required. Identifiers such as equipment model designation, trade name, military project code name, geographic location may also be included. If possible keywords should be selected from a published thesaurus. e.g. Thesaurus of Engineering and Scientific Terms (TEST) and that thesaurus-identified. If it is not possible to select indexing terms which are Unclassified, the classification of each should be indicated as with the title.)

Time-Frequency Analysis
Discrete-time signal
Wigner Distribution
Generalized Likelihood Ratio Test
Fourier Transform
Radon Transform
Instantaneous Frequency
High-Frequency Radar
Doppler Processing
Accelerating Targets
Doppler Radar
Doppler Smearing
Generalized Velocity
Generalized Acceleration

Defence R&D Canada
is the national authority for providing
Science and Technology (S&T) leadership
in the advancement and maintenance
of Canada's defence capabilities.

R et D pour la défense Canada
est responsable, au niveau national, pour
les sciences et la technologie (S et T)
au service de l'avancement et du maintien des
capacités de défense du Canada.

www.drdc-rddc.dnd.ca